# Structural and Functional Characterization of Mycobactericidal Ubiquitin-Derived Peptides in Model and Bacterial Membranes

Marie H. Foss, Katelyn M. Powers, and Georgiana E. Purdy*

Department of Molecular Microbiology and Immunology, Oregon Health and Sciences University, Portland, Oregon 97239, United States

**ABSTRACT:** The mycobactericidal properties of macrophages include the delivery of bacteria to a hydrolytic lysosome enriched in bactericidal ubiquitin-derived peptides (Ub-peptides). To improve our understanding of interactions of ubiquitin-derived peptides with mycobacteria, we further characterized the structure and function of bactericidal Ub-peptide Ub2. We found that Ub2 adopts a $\beta$-sheet conformation in the context of sodium dodecyl sulfate micelles and phospholipid (1:1 1-palmitoyl-2-oleoyl-*sn*-glycero-3-phosphoglycerol/1-palmitoyl-2-oleoyl-*sn*-glycero-3-phosphatidylcholine) vesicles that was dependent upon the primary sequence of the peptide. Point mutations in Ub2 that reduced the net charge of the peptide decreased Ub2 bactericidal activity. We investigated Ub-peptide function in the context of model membranes and intact bacteria. Differential scanning calorimetry analysis demonstrated that Ub2 inserts into and perturbs model phospholipid vesicles. In addition, we demonstrate that Ub2 disrupts the integrity of the mycobacterial membrane, equilibrates the transmembrane potential, and is localized within both the mycobacterial membrane and cytoplasm of treated bacteria. Finally, we identified additional bactericidal Ub-peptides and characterized their activity and structure. This study provides new insight into the mycobactericidal mechanisms of Ub-peptides.
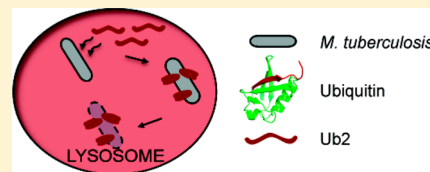
*Mycobacterium tuberculosis* is an intracellular pathogen that infects one-third of the world population, with 2 million TB-related deaths reported annually.[1] In the macrophage, *M. tuberculosis* survives by arresting phagosome maturation and blocking fusion of the bacterium-containing vacuole with the lysosome. However, in activated or autophagic macrophages, mycobacteria are delivered to the lysosome and killed.[2−4] We found that ubiquitin-derived peptides (Ub-peptides) contribute to the mycobactericidal activity of the lysosome and subsequently showed that immunodepletion of ubiquitin from the lysosomal extract results in reduced bactericidal activity.[3,5] While full-length ubiquitin lacks bactericidal activity, Ub-peptides obtained in vitro via digestion of ubiquitin by cathepsin proteases effectively kill mycobacteria. Combined, these data suggest that ubiquitylated proteins are delivered to the lysosomal compartment, where cathepsin proteases release Ub-peptides that possess antimicrobial activity.[6]

Our subsequent efforts have focused on characterizing the mycobactericidal activity of Ub-peptides. Many of these studies use the mycobactericidal ubiquitin-derived peptide Ub2 (STLHLVLRLRGG). Using kinetic fluorometric assays, we previously showed that Ub2 targets and reduces mycobacterial membrane integrity.[5] On the basis of these results, we hypothesized that Ub-peptides act like other characterized host antimicrobial peptides that are key components of the host innate immune response. These peptides are thought to target and damage the microbial membrane, although some may possess additional bactericidal activities.[7,8] Biophysical studies of antimicrobial peptides using model membranes have revealed diverse structures and suggest several potential mechanisms for membrane permeabilization. For example, the antimicrobial peptide LL-37 adopts an $\alpha$-helical con-

formation and likely disrupts bacterial membranes by initially "carpeting" the surface of the membrane and then inserting at the polar−nonpolar interface of the membrane. In support of this model, differential scanning calorimetry (DSC) analysis demonstrated that LL-37 interacts with and alters the thermodynamic properties of model lipid bilayers.[9] To further understand the mechanism by which Ub-peptides function, we used biochemical approaches to define the Ub2 structure−function relationship and identify biologically relevant Ub-peptides. We found that the primary sequence of Ub2 is vital to Ub2 secondary structure, membrane targeting ability, and bactericidal activity. In addition, we demonstrate that Ub2 is localized within the mycobacterial membrane and cytoplasm. Finally, additional bactericidal Ub-peptides were identified and their bactericidal activities and structures characterized.

## ■ EXPERIMENTAL PROCEDURES

**Maintenance of Bacterial Cultures.** *Mycobacterium smegmatis* mc²155 and *Mycobacterium bovis* BCG (Pasteur) were maintained in Middlebrook 7H9 medium (Difco) or on Middlebrook 7H11 agar (Difco) plates supplemented with ADS. *Bacillus megaterium* 899 was obtained from John Helmann at Cornell University (Ithaca, NY). *Escherichia coli* DH5α and *B. megaterium* were routinely cultured in Luria broth and LB agar plates.

**Antimicrobial Peptides.** Ub-peptides were synthesized by GenScript (Piscataway, NJ) with purities of >90%. Lyophilized

peptide aliquots were stored at −80 °C. Peptides were resuspended in deionized $H_2O$ (d$H_2O$) at 1 mM and used immediately. LL-37 was purchased from Anaspec (Fremont, CA).

**Circular Dichroism.** Circular dichroism (CD) spectra of Ub-peptides were recorded on a 215 CD spectrometer (Aviv Instruments Inc.). The lipids 1-palmitoyl-2-oleoyl-*sn*-glycero-3-phosphoglycerol (POPC) and 1-palmitoyl-2-oleoyl-*sn*-glycero-3-phosphatidylcholine (POPG) were purchased from Avanti Polar Lipids, Inc. (Alabaster, AL). POPC and POPG were mixed at a 1:1 molar ratio and dried under a stream of nitrogen. The POPC/POPG mixture was resuspended in 10 mM Tris-HCl (pH 7.4) and sonicated for 45 min at 40 °C to form vesicles. Ub-peptides were added at a final concentration of 100 $\mu$M in d$H_2O$ to 100 mM sodium dodecyl sulfate (SDS) or 470 $\mu$M POPC/POPG vesicles (1:1). CD measurements were taken with a 0.1 cm path-length QS cuvette (Hellma Analytics). Spectra were recorded at 4 °C from 260 to 190 nm, measuring in 0.5 nm steps. The average of triplicate recordings was graphed.

**Bactericidal Assays.** To determine the antimicrobial activity of Ub-peptides against *M. smegmatis*, *B. megaterium*, and *E. coli*, bacteria were normalized to densities of $5 \times 10^5$ colony-forming units/mL in 7H9 medium or Luria broth and treated with 2-fold dilutions of peptide overnight at 37 °C. The number of surviving bacteria was determined by plating serial dilutions on 7H11 or LB agar plates. MICs were calculated and are defined as the minimal concentration resulting in ≥90% decreased bacterial viability.

**Differential Scanning Calorimetry.** The lipids 1,2-dimyristoyl-*sn*-glycero-3-phosphocholine (DMPC), 1,2-dimyristol-*sn*-glycero-3-[phospho-*rac*-(1-glycerol)] (DMPG), and 1,2-dipalmitoleoyl-*sn*-glycero-3-phosphoethanolamine (Di-PoPE) were purchased from Avanti Polar Lipids, Inc. DMPC and DMPG were mixed in a 1:1 molar ratio in glass tubes and the solvent dried from lipids under a stream of nitrogen. DMPC/DMPG samples were resuspended to a concentration of 2.5 mg/mL in buffer containing 20 mM HEPES and 100 mM NaCl (pH 7.0) in the presence or absence of peptide. DMPC/DMPG samples were heated to 50 °C in a water bath for 2 min and then vortexed for 30 s. Heating and vortexing of samples were repeated a total of three times to form multilamellar lipid vesicles. Samples were degassed under vacuum for 15 min after being cooled to room temperature. Samples were loaded into an Applied Thermodynamics N-DSC II instrument at 10 °C, heated in the cell to 40 °C, and cooled to 10 °C before being scanned. Samples were scanned from 5 to 40 °C at a rate of 1 °C/min, and a buffer scan was subtracted for baseline correction. We measured the main phase transition temperature of lipids using Cpcalc version 2.2 from Calorimetry Sciences Corp.

For DiPoPE samples, lipids were dried in glass tubes under a stream of nitrogen and resuspended to a concentration of 10 mg/mL in buffer containing 10 mM Tris, 100 mM NaCl, 1 mM EDTA, and 0.002% $NaN_3$ (pH 7.4) in the presence or absence of peptide. Multilamellar lipid vesicles were prepared and degassed as described previously, but with a 60 °C water bath. Samples were loaded into the cell at 25 °C, heated to 60 °C, and cooled to 10 °C before being scanned. Samples were scanned twice from 10 to 60 °C at a rate of 1 °C/min, and a buffer scan was subtracted for baseline correction of data. We measured the $L_\alpha$ to $H_\parallel$ phase transition temperature as described above.

**Measurement of ΔΨ Equilibration in Mycobacteria.** Equilibration of the transmembrane potential (ΔΨ) was assessed by labeling *M. smegmatis* mc$^2$155 and *M. bovis* BCG with 3,3′-diethyloxacarbocyanine iodide (DiOC$_2$) (Molecular Probes, Eugene, OR) in PBS supplemented with 50 mM $K_2SO_4$ (pH 7.2). Mycobacteria were washed with buffer, stained with 30 $\mu$M DiOC$_2$ in buffer for 5 min, washed, and resuspended in buffer until the OD$_{600}$ reached 0.2. Cells were treated in triplicate with d$H_2O$, DMSO, 50 $\mu$M Ub2, or 50 $\mu$M carbonyl cyanide *m*-chlorophenylhydrazone (CCCP) as a control for ΔΨ dissipation. Fluorescence emission for DiOC$_2$ was measured using a Gemini EM fluorescence microplate reader (Molecular Devices, Sunnyvale, CA) at 612 and 538 nm using an excitation wavelength of 485 nm after a 30 min incubation. The DiOC$_2$ red:green fluorescence ratio was calculated by dividing the fluorescence intensity at 612 nm by that at 538 nm.

**Evaluation of Membrane Leakage by Diffusion of a Vesicle-Encapsulated Fluorophore.** The ability of Ub2 and Ub2 point substitution peptides to disrupt model bacterial membranes was determined by the encapsulation of carboxyfluorescein in POPC/POPG (1:1) vesicles according to previously established methods with some modification.[10] Lipids were hydrated at a concentration of 10 mM in buffer containing 10 mM Tris (pH 7.4), 0.1 mM EDTA, and 50 mM carboxyfluorescein. The encapsulation of the fluorophore in large unilamellar vesicles (LUVs) was performed via a 20 min sonication in a Branson 2510 sonicator followed by snap-freezing in a dry ice/ethanol bath, which was repeated a total of four times. Vesicles were separated from nonencapsulated dye by being passed through a Sephadex column.[11] The filtered vesicles containing carboxyfluorescein were diluted to 50 $\mu$M lipid with 10 mM Tris (pH 7.4), 0.1 mM EDTA, and 100 mM KCl. The diluted vesicles were treated with 10 $\mu$M peptide, and the equilibration of fluorescence was monitored using a Gemini EM fluorescence microplate reader. After 30 min, the fluorescence of each sample was recorded and the fluorescence of d$H_2O$-treated vesicles subtracted. The release of dye from vesicles by peptides was compared to that from vesicles treated with 0.01% Triton X-100, which dissolves vesicles and releases the encapsulated dye.

**Subcellular Fractionation and Western Blot Analysis.** *M. smegmatis* mc$^2$155 was treated with 50 $\mu$M Ub2-biotin or buffer control for 1 h before bacterial cultures were harvested. To determine the localization of Ub2, subcellular fractions were obtained by differential centrifugation.[12] Briefly, cells were washed with PBS and resuspended at an OD$_{600}$ of 10 in PBS containing protease inhibitors (Complete Protease Inhibitor Cocktail, Roche) and then broken by bead beating with 0.1 mm glass beads for 1 min. Unbroken cells were pelleted at 3000*g*, and the supernatant was retained as total lysate. The total lysate was ultracentrifuged at 27000*g* for 1 h at 4 °C. The pellet was saved as the cell wall. The supernatant was centrifuged at 100000*g* for 1 h at 4 °C to separate the cytoplasm (supernatant) from the cell membrane (pellet). Equivalent amounts of membrane and cytoplasmic fractions were applied to nitrocellulose using a slot blotter. Western analysis was performed using a monoclonal antibody against biotin (Abcam Inc.), a polyclonal antibody against membrane protein Ag85, and monoclonal antibody IT-42 against cytoplasmic protein KatG. The antibody against Ag85 and KatG were obtained from BEI Resources (Manassas, VA). The HRP-conjugated secondary antibody was used at a 1:10000 dilution.
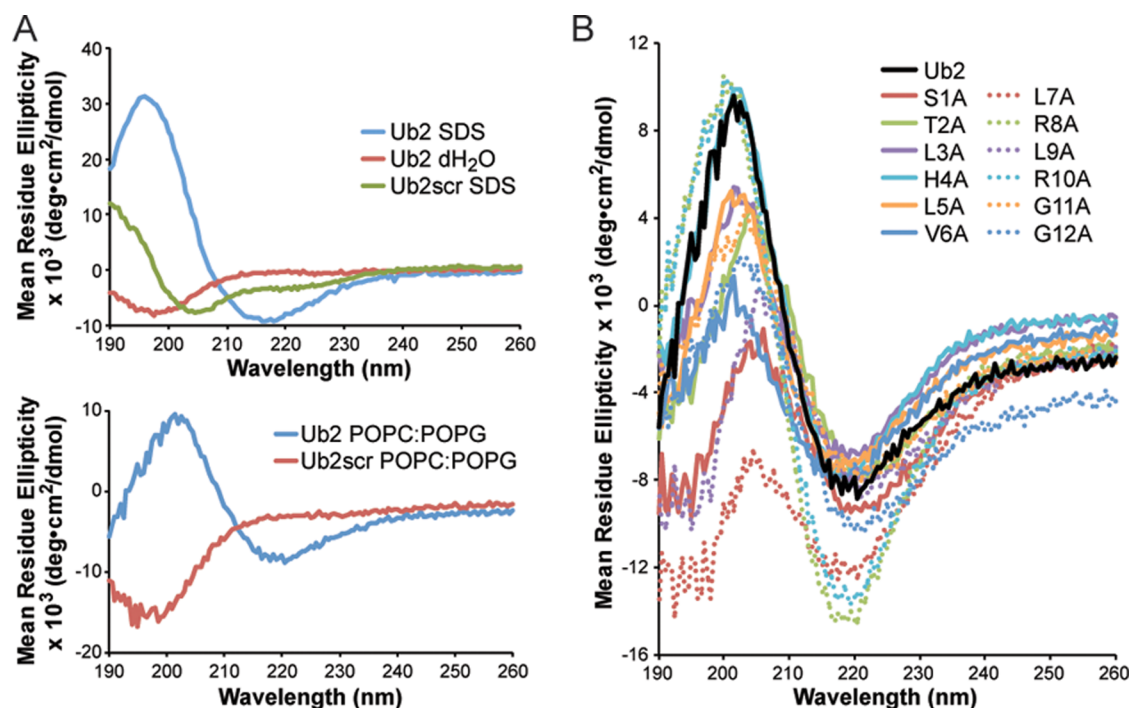
**Figure 1.** Ub2 adopts a $\beta$-sheet structure in membrane mimetics that depends on primary amino acid sequence. (A) Circular dichroism (CD) spectra of 100 $\mu$M Ub2 (STLHLVLRLRGG) or Ub2scr (RLGRLVSLHTLG) were measured in the presence and absence of 100 mM SDS (top) or 470 $\mu$M POPC/POPG vesicles (bottom). (B) CD spectra of 100 $\mu$M Ub2 point substitution peptides in the presence of 470 $\mu$M POPC/POPG vesicles were indicative of $\beta$-sheet structure.

**Table 1. MICs of Ub2 and Ub2 Point-Substituted Peptides against *M. smegmatis*, *B. megaterium*, and *E. coli***

| peptide | sequence (charge) | MIC ($\mu$M) | | |
|---|---|---|---|---|
| | | *M. smegmatis* | *B. megaterium* | *E. coli* |
| Ub2 | STLHLVLRLRGG (+3) | 50 | 5 | 10 |
| Ub2scr | RLGRLVSLHTLG (+3) | >400 | >100 | >100 |
| Ub2$_{S1A}$ | ATLHLVLRLRGG (+3) | 25 | 5 | 10 |
| Ub2$_{T2A}$ | SALHLVLRLRGG (+3) | 50 | 50 | >100 |
| Ub2$_{L3A}$ | STAHLVLRLRGG (+3) | 100 | 50 | >100 |
| Ub2$_{H4A}$ | STLALVLRLRGG (+2) | >400 | 10 | 10 |
| Ub2$_{L5A}$ | STLHAVLRLRGG (+3) | 50 | 50 | 5 |
| Ub2$_{V6A}$ | STLHLALRLRGG (+3) | 25 | 50 | >100 |
| Ub2$_{L7A}$ | STLHLVARLRGG (+3) | 100 | 50 | >100 |
| Ub2$_{R8A}$ | STLHLVLALRGG (+2) | >400 | 100 | >100 |
| Ub2$_{L9A}$ | STLHLVLRARGG (+3) | 50 | 50 | 50 |
| Ub2$_{R10A}$ | STLHLVLRLAGG (+2) | >400 | >100 | >100 |
| Ub2$_{G11A}$ | STLHLVLRLRAG (+3) | >400 | 50 | >100 |
| Ub2$_{G12A}$ | STLHLVLRLRGA (+3) | >400 | 50 | >100 |

**High-Performance Liquid Chromatography (HPLC) and Mass Spectrometry Analysis.** HPLC fractionation and mass spectrometry analysis were performed to identify biologically relevant Ub-peptides. Two milligrams of purified ubiquitin (Sigma) was digested by cathepsin L protease (Biomol). Digested ubiquitin was separated by HPLC on a C18 reverse phase column using an acetonitrile gradient. Each fraction was evaluated by bactericidal assays as described above. Peptides in the fractions that resulted in >90% reduction in *M. smegmatis* viability were identified by mass spectrometry.

**CMFDA Assay for Measuring the pH of the Bacterial Cytoplasm.** Membrane integrity was assessed by labeling *M. smegmatis* mc²155 with 5'-chloromethylfluorescein diacetate (CMFDA) (Molecular Probes) in PBS (pH 7.2). Bacteria were washed twice in PBS (pH 7) before being resuspended at an

OD$_{600}$ of 1.5 in PBS (pH 5.5) and transferred to a 96-well microplate. Fluorescence emission was measured at 520 nm using excitation wavelengths of 450 and 490 nm in a SpectraMax Gemini EM fluorescent plate reader for 10 min (Molecular Devices, Sunnyvale, CA). Ub-peptides were used at a concentration of 100 $\mu$M. Conversion of the excitation ratio to pH was achieved through polynomial regression of a standard curve generated by treating CMFDA- labeled bacteria with 10 $\mu$M nigericin in buffers of known pH. The assay was performed in triplicate, and the average pH of the bacterial cytoplasm after nigericin and Ub-peptide treatment is presented graphically.
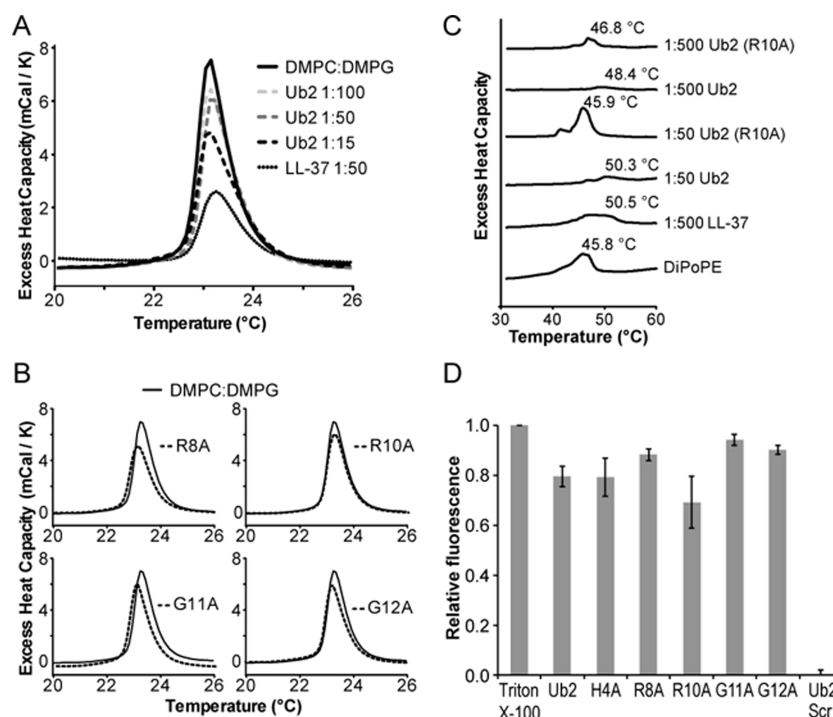
**Figure 2.** Perturbation of membrane properties by Ub2 and point substitution peptides. (A) Phase transition temperatures of DMPC/DMPG (1:1) multilamellar vesicles in the presence and absence of Ub2. Ub2 was added to DMPC/DMPG (1:1) vesicles at the indicated peptide:lipid proportions. Addition of LL-37 or Ub2 perturbs the main phase transition peak height, suggesting insertion into the vesicles. (B) Ub2 point substitution peptides were added to DMPC/DMPG (1:1) vesicles at a peptide:lipid ratio of 1:50. The addition of nonbactericidal Ub2 point substitution peptides reduced the enthalpy of the phase transition temperature. (C) Phase transition temperatures of DiPoPE in the presence and absence of Ub-peptides. The addition of LL-37 or Ub2 increases the temperature required for the phase transition of DiPoPE, suggesting the peptides prevent the $L_\alpha-H_{||}$ transition. (D) Relief of carboxyfluorescein self-quenching by disruption of dye encapsulation in large unilamellar POPC/POPG (1:1) vesicles. Carboxyfluorescein-containing POPC/POPG (1:1) vesicles were incubated in the presence of either 10 $\mu$M Ub-peptides or 0.01% Triton-X. Relative fluorescence is defined as the fluorescence of peptide-treated samples relative to that of detergent-released carboxyfluorescein. The averages ± standard deviations from three independent assays are shown.

## ■ RESULTS

**Ub2 Adopts a $\beta$-Sheet Structure under Membrane Mimicking Conditions.** Host antimicrobial peptides adopt a number of conformations, including $\alpha$-helices, relaxed coils, and antiparallel $\beta$-sheets. To determine the secondary structure of the antimicrobial peptide Ub2, we performed circular dichroism (CD). Initial CD measurements indicated Ub2 was largely unstructured in aqueous solution (Figure 1A). It is possible that Ub2 is primarily disordered in the aqueous environment but adopts a stable conformation upon interaction with the bacterial membrane. This context-dependent shift in conformation would be consistent with that observed in other antimicrobial peptides. Notably, histone-derived antimicrobial peptides lacked structure in aqueous solution but acquire a stable structure under membrane mimetic conditions.[13] We therefore performed CD of Ub-peptides in the presence of membrane mimetics. In the presence of SDS micelles or POPC/POPG vesicles, Ub2 produced a negative peak at 220 nm and a positive peak at 197 nm, consistent with a $\beta$-sheet secondary structure (Figure 1A).

**Ub2 Function and Structure Depend on the Primary Amino Acid Sequence.** To determine whether the primary sequence of Ub2 was important for Ub2 function or structure, we generated the Ub2scr peptide (RLGRLVSLHTLG) that has a scrambled amino acid sequence relative to that of Ub2 (STLHLVLRLRGG). Ub2scr lacked bactericidal activity against *M. smegmatis* mc²155 (Table 1). To determine whether

it still adopted a $\beta$-sheet in the context of a membrane mimetic, we performed CD on the Ub2scr peptide in the presence of SDS or POPC/POPG vesicles. Unlike Ub2, Ub2scr did not adopt a $\beta$-sheet structure and instead appeared to be slightly $\alpha$-helical in SDS or unordered in POPC/POPG vesicles (Figure 1A). These data suggested that the primary amino acid sequence of Ub2 is important for both bactericidal activity and secondary structure.

To further define the important residues for Ub2 structure and function, we performed scanning alanine mutagenesis on the Ub2 peptide. Twelve Ub2 point-substituted peptides were synthesized, and bactericidal assays were performed to identify key amino acid residues for Ub2 function. Point substitutions that reduced the positive charge of Ub2 (Ub2$_{H4A}$, Ub2$_{R8A}$, and Ub2$_{R10A}$) and peptides with altered C-terminal residues (Ub2$_{G11A}$ and Ub2$_{G12A}$) were not bactericidal against *M. smegmatis* (Table 1). The Ub2$_{S1A}$ and Ub2$_{V6A}$ peptides had reduced MICs against *M. smegmatis* compared to that of Ub2. Ub2$_{L3A}$ and Ub2$_{L7A}$ had higher MIC values than Ub2 but still retained activity against *M. smegmatis*. We also determined the MICs of the Ub2 peptides against the Gram-negative species *E. coli* and the Gram-positive species *B. megaterium* (Table 1). Consistent with our results with *M. smegmatis*, we found that Ub2scr lacked activity against *E. coli* and *B. megaterium*. Ub2$_{R8A}$, Ub2$_{R10A}$, Ub2$_{G11A}$, and Ub2$_{G12A}$ also had reduced bactericidal activity against both species. However, Ub2$_{H4A}$ retained much of its activity against *E. coli* and *B. megaterium*, suggesting that a charged residue at this location of the peptide is more

**Table 2. Effect of Ub2 on the Mycobacterial Transmembrane Potential**

| | DiOC$_2$ red:green fluorescence ratio | | | |
| --- | --- | --- | --- | --- |
| strain | DMSO | CCCP | dH$_2$O | Ub2 |
| *M. smegmatis* | 0.103 ± 0.002 | 0.039 ± 0.002 | 0.099 ± 0.001 | 0.048 ± 0.001 |
| *M. bovis* | 0.112 ± 0.001 | 0.086 ± 0.003 | 0.109 ± 0.003 | 0.042 ± 0.002 |

important for function against mycobacteria than other species. To determine whether specific amino acid residues were important for Ub2 structure, CD spectrometry was performed using POPC/POPG vesicles. All Ub2 point substitution peptides retained a *β*-sheet structure, though the total *β*-sheet composition presented by alanine-substituted peptides (especially S1A, L7A, and L9A) is not identical to that of Ub2 (Figure 1B). These results indicate that Ub2 structure does not depend on a single residue and that peptide structure alone does not confer bactericidal activity. However, peptide activity does depend on the charge of the peptide, suggesting that electrostatic interactions occur between the peptide and the bacterial membrane.

**Ub2 Affects Membrane Structure and Integrity.** Our working model is that Ub2 peptides target and damage the inner bacterial membrane. Differential scanning calorimetry (DSC) can be used to demonstrate interactions between antimicrobial peptides and lipids in terms of changes in the thermodynamic phase transition of model lipids. To determine if Ub2 function involves perturbation of membrane properties, we performed DSC on multilamellar vesicles composed of DMPC and DMPG (1:1) or DiPoPE. As a control, we included antimicrobial peptide LL-37 that is known to reduce the enthalpy ($\Delta H$) of the gel lamellar (L$\beta$) to fluid lamellar (L$_\alpha$) phase transition of DMPC/DMPG vesicles.[14] We observed a sharp peak for the lipid alone at 23.3 °C; its amplitude was reduced upon addition of increasing concentrations of Ub2. This result indicates that Ub2 reduces the enthalpy of the L$\beta$–L$_\alpha$ phase transition (Figure 2A). While Ub2 incorporation perturbed the shape of the main phase transition temperature peak, higher concentrations of Ub2 were required to achieve this versus those for LL-37. DSC was also used to determine if the nonbactericidal Ub2 point substitution peptides were able to target membranes and perturb their thermodynamic properties. Reduced enthalpy upon treatment of DMPC/DMPG vesicles with Ub2$_{R8A}$, Ub2$_{R10A}$, Ub2$_{G11A}$, and Ub2$_{G12A}$ in DMPC/DMPG membranes indicates that these peptides also incorporate and reduce the enthalpy of the phase transition (Figure 2B).

We also examined the ability of Ub2 to insert into DiPoPE liposomes by DSC. DiPoPE undergoes the fluid lamellar (L$_\alpha$) to inverted hexagonal (H$_{||}$) phase transition at 45.8 °C. Addition of Ub2 restricts the transition to H$_{||}$ and induces positive curvature strain (Figure 2C). However, we also noted that a 10-fold greater amount of Ub2 was required to achieve a shift in the transition temperature equivalent to that of LL-37. These data obtained with model lipid bilayers suggest that in the context of a membrane, Ub2 incorporates into the hydrophobic core of the membrane and perturbs them. Using the DiPoPE liposomes, we again investigated the membrane targeting properties of a nonbactericidal Ub2 point-substituted peptide. We found that Ub2$_{R10A}$ peptide did not increase the phase transition temperature to the same extent as equivalent amounts of Ub2. This result suggests that in the context of these membrane conditions, Ub2$_{R10A}$ is less able to insert and induce curvature in DiPoPE membranes.

To determine whether Ub-peptide treatment results in increased membrane permeability, we performed a dye leakage assay. POPC/POPG (1:1) liposomes containing carboxyfluorescein at a self-quenching concentration were prepared. Relief of carboxyfluorescein self-quenching upon treatment with Ub2 and inactive Ub2 point substitution peptides was measured and expressed as fluorescence relative to vesicles lysed with detergent. Addition of the Ub2scr peptide resulted in no dye leakage, and the result was statistically equivalent to that for dH$_2$O-treated vesicles. Addition of Ub2 and nonbactericidal Ub2 point substitution peptides resulted in increased fluorescence consistent with release of carboxyfluorescein (Figure 2D). These data suggest that structured, biologically inactive Ub-peptides are still able to interact with model membranes but in the context of bacteria are deficient in reaching or effectively interacting with the bacterial membrane.

**Ub2 Equilibrates ΔΨ across Mycobacterial Membranes.** Our previous work demonstrated that treatment of mycobacteria with Ub-peptides results in the equilibration of the external and internal pH.[5] To further understand the consequences of Ub-peptide damage, we performed an additional fluorescence assay using the fluorophore DiOC$_2$ to measure the transmembrane potential (ΔΨ) of mycobacteria upon Ub2 treatment. This assay utilizes the charge-sensitive properties of DiOC$_2$ whose red:green fluorescence emission ratio is greater when the dye is associated with the negatively charged internal bacterial membrane. Dissipation of ΔΨ results in lower red:green emission ratios. The intact ΔΨ of control *M. smegmatis* mc$^2$155 treated with either DMSO or dH$_2$O yielded an emission ratio of 0.103 ± 0.002 or 0.099 ± 0.001, respectively (Table 2). Following a 30 min treatment with 50 μM CCCP or 50 μM Ub2, the emission ratio was reduced to 0.039 ± 0.002 or 0.048 ± 0.001, respectively. This reduction of the red:green emission ratio upon Ub2 treatment indicates a loss of ΔΨ across the membrane. We found the same result for *M. bovis* BCG, for which we measured intact ΔΨ values for cells treated with DMSO (0.112 ± 0.001) and dH$_2$O (0.109 ± 0.003) and reduced ΔΨ values with 30 min CCCP (0.086 ± 0.003) and Ub2 (0.042 ± 0.002) treatments. Combined, our data demonstrate that Ub2 treatment not only results in the loss of ΔpH but also eliminates the ΔΨ in fast- and slow-growing mycobacteria.

**Ub-Peptides Are Localized to the Mycobacterial Membrane and Cytoplasm.** After insertion into the bacterial membrane, some host antimicrobial peptides translocate into the cytoplasm where they are proposed to have additional targets. Our previous membrane integrity studies suggested that Ub-peptides are localized to the bacterial membrane. To verify this localization and determine if Ub2 also accesses the cytoplasm, we performed subcellular localization studies. A biotinylated Ub2 peptide was synthesized, and the bactericidal activity was tested. The bactericidal activity of Ub2-biotin was similar to that of Ub2 (Figure 3A). Upon subcellular fractionation and Western blot analysis, we found Ub2-biotin in both the membrane and cytoplasmic fractions (Figure 3B). As a control for the purity of our fractions, we performed
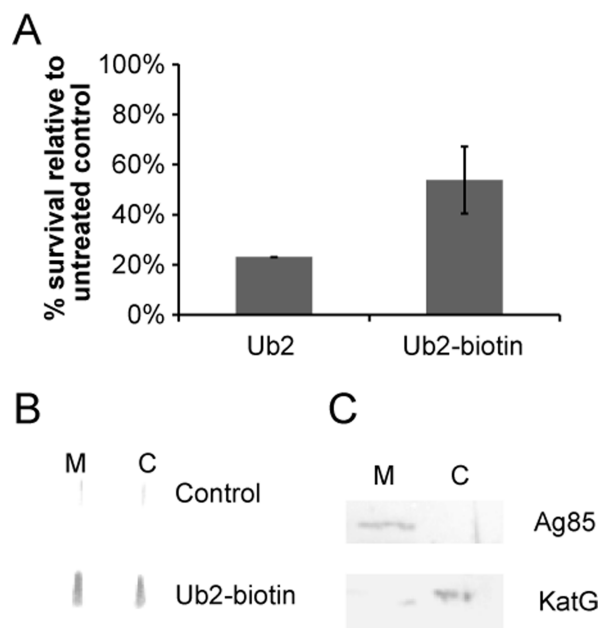
**Figure 3.** Subcellular localization of Ub2-biotin. (A) *M. smegmatis* mc²155 was subcultured to a density of $5 \times 10^5$ colony-forming units/mL in 7H9 medium containing 50 $\mu$M Ub2 or Ub2-biotin. Following overnight treatment, the number of viable bacteria was determined by plating serial dilutions, and the average of three replicates is shown. (B) *M. smegmatis* mc²155 was treated with 50 $\mu$M Ub2-biotin or buffer control. Bacteria were harvested, and membrane (M) and cytoplasmic (C) fractions were obtained and applied to nitrocellulose using a slot blotter. Western analysis was performed with the monoclonal antibody against biotin. (C) To assess the purity of the subcellular fractionation protocol, membrane and cytoplasmic fractions were resolved on a 12% sodium dodecyl sulfate—polyacrylamide gel electrophoresis gel and Western analysis was performed using antibodies against the Ag85 membrane protein and cytoplasmic protein KatG.

Western analysis using antibodies against known membrane and cytoplasmic proteins. This analysis ruled out significant contamination of our fractions and supports localization of Ub2-biotin to both the membrane and cytoplasm (Figure 3C).

**Biologically Relevant Ub-Peptides Were Isolated.** We investigated the existence of other biologically relevant Ub-peptides, as many diverse Ub-peptides can be generated as a result of cathepsin proteolysis of ubiquitylated proteins. Full-length ubiquitin was digested with cathepsin L protease, and the resulting Ub-peptides were separated by HPLC. Each fraction was collected and tested for bactericidal activity (data not shown). Mass spectrometry identified the Ub-peptides present in each of the bactericidal fractions. Multiple peptides were identified in some bactericidal fractions, for example, Ub17.1 and Ub17.2. To confirm the bactericidal activity of the novel Ub-peptides, we tested synthetic peptides against *M. smegmatis*, *B. megaterium*, and *E. coli*. Ub17.1 (KTLTGKTIT-LE) and Ub21 (EVEPSDTIENVKAKIQ) exhibited bactericidal activity against *M. smegmatis* and *E. coli* comparable to that of Ub2 (Table 3). To determine if the $\beta$-sheet structure is a shared property of bactericidal Ub-peptides, we performed CD spectroscopy. CD spectral measurements of Ub17.1 were consistent with unordered secondary structure, whereas Ub21 exhibited CD spectral measurements associated with $\alpha$-helices (Figure 4A).

We previously showed that Ub2 reduces the $\Delta$pH of the *M. smegmatis* membrane integrity using an assay based upon the

**Table 3. MICs of Biologically Relevant Ub-Peptides**

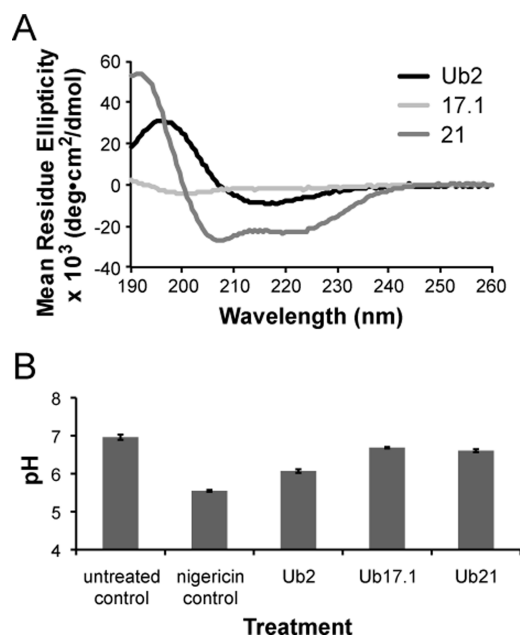| peptide | sequence | MIC ($\mu$M) | | |
|---|---|---|---|---|
| | | *M. smegmatis* | *B. megaterium* | *E. coli* |
| 17.1 | KTLTGKTITLE | 50 | >100 | 10 |
| 21 | EVEPSDTIENVKAKIQ | 50 | >100 | 10 |



**Figure 4.** Secondary structure and activity of biologically relevant peptides. (A) Secondary structures of bactericidal Ub-peptides Ub17.1 and Ub21 determined by CD spectrometry. Peptides were analyzed at 100 $\mu$M in the presence of 100 mM SDS. (B) CMFDA-labeled *M. smegmatis* was resuspended in PBS (pH 5.5) and treated with nigericin or 100 $\mu$M Ub-peptide. Fluorescence emission at 520 nm was measured at excitation wavelengths of 450 and 490 nm, and the excitation ratio was converted to pH by regression. The averages ± standard deviations from three assays are shown.

pH-sensitive fluorophore carboxyfluorescein (CMFDA).[5] CMFDA is a membrane-permeable probe, which is processed into a membrane-impermeable form after uptake. The fluorescence emission of fluorescein at 520 nm is pH-sensitive upon excitation at 490 nm but is pH-insensitive upon excitation at 450 nm. CMFDA-labeled *M. smegmatis* was resuspended in pH 5.5 buffer and treated with Ub-peptides. Membrane integrity is evaluated by the shift in fluorescence upon exposure of the intracellular fluorophore to the extracellular pH. To determine whether Ub17.1 and Ub21 possessed membrane damaging properties, we performed the CMFDA fluorimetric assay on *M. smegmatis*. While there was a decrease observed in the cytoplasmic pH following treatment with Ub17.1 and Ub21, membrane integrity was not compromised to the same extent as it was upon treatment with Ub2 (Figure 4B). These results suggest the mechanism of action or efficiency of these peptides differs from that of Ub2. It is possible that these peptides either disrupt the membrane transiently or require more time than Ub2 to cause equivalent membrane damage.

■ **DISCUSSION**

Our previous studies showed Ub-peptides contribute to the lysosomal killing of *M. tuberculosis*.[5] This novel finding greatly impacts our knowledge of the host antimicrobial repertoire and

the immune control of mycobacterial infections. To improve our understanding of the bactericidal mechanism of Ub-peptides, we further characterized the structure and function of model Ub-peptide Ub2 and identified two novel biologically relevant Ub-peptides. Using CD, we found that Ub2 adopts a $\beta$-sheet structure in the context of membrane mimetic SDS micelles and POPG/POPC (1:1) liposomes. When the amino acids of Ub2 are scrambled, the peptide loses ordered structure and bactericidal function. This is not without precedent as previous work demonstrated that some but not all Bac2A scrambled peptides lose bactericidal activity.[15]

We next determined which amino acids are important for Ub2 bactericidal activity and structure using alanine scanning mutagenesis. Ub2$_{H4A}$, Ub2$_{R8A}$, Ub2$_{R10A}$, Ub2$_{G11A}$, and Ub2$_{G12A}$ were not bactericidal against *M. smegmatis*, indicating that the crucial residues of Ub2 for bactericidal activity are charged or positioned at the C-terminal end of the peptide. The importance of positive charge for bactericidal function of Ub2 is consistent with the proposed model for cationic antimicrobial peptides that are thought to initially interact with bacterial membranes via electrostatic interactions. In addition, DSC analysis of nonbactericidal peptides in the context of DiPoPE liposomes demonstrated that Ub2$_{R10A}$ was unable to stabilize positive curvature as robustly as Ub2, suggesting that the loss of charge results in a peptide that fails to establish the same stable lipid–peptide interactions as Ub2. The peptides with reduced positive charge remain structured and able to disrupt artificial membranes as assessed by membrane leakage, so it is possible that these peptides lack bactericidal activity because they either have poor access to the bacterial membrane or are unable to stably insert. Alternatively, our in vitro studies may not provide the correct lipid environment for discerning differences in activity between Ub2 and alanine-substituted peptides. The inner membrane of mycobacteria is compositionally similar to the membranes of other species of bacteria,[16] and Ub2 is bactericidal against multiple species. Therefore, we used phospholipids that are commonly used to model bacterial membranes but acknowledge that others have demonstrated that lipid composition can significantly impact peptide function.[17] Ub2$_{G11A}$ and Ub2$_{G12A}$ also lacked bactericidal activity, but the underlying reason for this phenotype is less clear. The requirement of glycine for function at these positions suggests the necessity of flexibility or tight packing at the C-terminus. It is possible that the C-terminal glycines are required for formation of a cap, which folds back to make contacts and stabilize the peptide in a $\beta$-sheet structure. A C-terminal glycine appears to stabilize the $\alpha$-helical structure of pleurocidin and enhance bactericidal activity.[18]

On the basis of our previous work and the data presented here, we propose a model in which a key attribute of Ub2 is its ability to interact with and disrupt the mycobacterial membrane. Using fluorimetric assays of intact mycobacteria, we showed previously that treatment with Ub2 results in the equilibration of the external and internal pH,[5] and we report here the loss of transmembrane potential. These studies are complemented with differential scanning calorimetry and dye encapsulation assays performed on model liposomes. Similar to the well-characterized antimicrobial peptide LL-37, Ub2 reduced the phase transition of DMPC/DMPG liposomes and increased the $L_\alpha$–$H_\parallel$ phase transition temperature of DiPoPE liposomes. We did note that LL-37 was more robust in these assays and that 10-fold higher levels of Ub2 were required to achieve the same effect. Using POPC/POPG liposomes

preloaded with carboxyfluorescein, we found that Ub2 treatment disrupts the membrane sufficiently to result in dye leakage and dequenching that is measured in terms of increased fluorescence. We confirmed the membrane targeting and insertion ability of Ub2 relative to mycobacteria by performing subcellular fractionation of *M. smegmatis* upon treatment with a biotinylated Ub2. Combined, our data demonstrate that Ub2 inserts into membrane environments, including bacterial membranes, and disrupts them to the extent that internal contents are released. Loss of membrane integrity in harsh environments such as the lysosome likely exposes the bacterium to adverse conditions, including additional bactericidal molecules.

Several mechanisms are proposed for the incorporation of an antimicrobial peptide into the bacterial membrane and access to the cytoplasm.[7,8] Peptides are thought to initially interact with the membrane electrostatically, inserting parallel to the membrane. This interaction may itself result in transient or sustained disruption of the membrane by interfering with lipid organization and/or packing. In the "carpet" model, the antimicrobial peptide coats the bacterial membrane surface to the extent that the peptides collapse inward, destroying the cytoplasmic membrane.[19] In the pore forming model, a high local concentration of peptide results in reorganization of the peptide perpendicular to the membrane and the formation of pores where the peptide forms the channel in a manner similar to the staves of a barrel.[20,21] In the case of short peptides like Ub2 that are unable to span the membrane, the micellar aggregate channel model is a more likely mechanism. This model proposes that high local concentrations of a peptide induce the cytoplasmic membrane to form micellar-like structures that effectively generate channels in the membrane.[22−24] Our subcellular localization data indicate that Ub2 not only inserts into the bacterial membrane but also reaches the cytoplasm. Other antimicrobial peptides that possess additional targets, including macromolecule biosynthesis, have been identified and their activities characterized.[25−27] In light of our data that show that nonbactericidal Ub2 point-substituted peptides retained membrane targeting capacity, we have not ruled out metabolic processes or bacterial enzymes as the secondary targets of Ub-peptides.

The lysosome is a highly toxic environment characterized by low pH and enriched with hydrolytic enzymes. Recently, the mycobactericidal contribution of antimicrobial peptides generated in the lysosome was revealed.[3,5,28] Cathepsin cleavage of proteins generates random peptides, and it is possible that the lysosome contains multiple bactericidal Ub-peptides. We identified additional bactericidal Ub-peptides from the in vitro digest of ubiquitin. Ub17.1 and Ub21 have lower net charges than Ub2 and exhibited unordered and $\alpha$-helical secondary structures, respectively. The Ub-peptides Ub17.1 and Ub21 showed little to no disruption of the mycobacterial membrane using the CMFDA assay. These results suggest Ub17.1 and Ub21 function in a manner distinct from that of Ub2, perhaps by targeting the membrane in a less disruptive manner. Therefore, it is likely that the lysosomal milieu contains a mixture of Ub-peptides that possess a range of structures and activities. Further characterization of these peptides may reveal mycobactericidal properties that can be enhanced or utilized to target mycobacteria and mycobacterial infections.

## AUTHOR INFORMATION

**Corresponding Author**

*Department of Molecular Microbiology and Immunology, Oregon Health and Sciences University, 3181 SW Sam Jackson Park Rd., Mail Code L220, Portland, OR 97239. Telephone: (503) 346-0767. Fax: (503) 494-6862. E-mail: purdyg@ohsu.edu.

**Notes**

The authors declare no competing financial interest.

## ACKNOWLEDGMENTS

## ABBREVIATIONS

Ub-peptides, ubiquitin-derived peptides; SDS, sodium dodecyl sulfate; DSC, differential scanning calorimetry; CD, circular dichroism; POPC, 1-palmitoyl-2-oleoyl-*sn*-glycero-3-phospho-glycerol; POPG, 1-palmitoyl-2-oleoyl-*sn*-glycero-3-phosphatidylcholine; DMPC, 1,2-dimyristoyl-*sn*-glycero-3-phosphocholine; DMPG, 1,2-dimyristoyl-*sn*-glycero-3-[phospho-*rac*-(1-glycerol)]; DiPoPE, 1,2-dipalmitoleoyl-*sn*-glycero-3-phosphoethanolamine; $\Delta\Psi$, transmembrane potential; $DiOC_2$, 3,3′-diethyloxacarbocyanine iodide; CCCP, carbonyl cyanide *m*-chlorophenylhydrazone; LUVs, large unilamellar vesicles; CMFDA, 5′-chloromethylfluorescein diacetate.

## REFERENCES

(1) World Health Organization (2010) Fact Sheet No. 104, who.int (accessed September 28).

(2) Schaible, U. E., Sturgill-Koszycki, S., Schlesinger, P. H., and Russell, D. G. (1998) Cytokine activation leads to acidification and increases maturation of *Mycobacterium avium*-containing phagosomes in murine macrophages. *J. Immunol. 160*, 1290−1296.

(3) Alonso, S., Pethe, K., Russell, D. G., and Purdy, G. E. (2007) Lysosomal killing of *Mycobacterium* mediated by ubiquitin-derived peptides is enhanced by autophagy. *Proc. Natl. Acad. Sci. U.S.A. 104*, 6031−6036.

(4) Gutierrez, M. G., Master, S. S., Singh, S. B., Taylor, G. A., Colombo, M. I., and Deretic, V. (2004) Autophagy is a defense mechanism inhibiting BCG and *Mycobacterium tuberculosis* survival in infected macrophages. *Cell 119*, 753−766.

(5) Purdy, G. E., Niederweis, M., and Russell, D. G. (2009) Decreased outer membrane permeability protects mycobacteria from killing by ubiquitin-derived peptides. *Mol. Microbiol. 73*, 844−857.

(6) Purdy, G. E. (2011) Taking Out TB-Lysosomal Trafficking and Mycobactericidal Ubiquitin-Derived Peptides. *Front. Microbiol. 2*, 7.

(7) Brogden, K. A. (2005) Antimicrobial peptides: Pore formers or metabolic inhibitors in bacteria? *Nat. Rev. Microbiol. 3*, 238−250.

(8) Hancock, R. E. W., and Sahl, H.-G. (2006) Antimicrobial and host-defense peptides as new anti-infective therapeutic strategies. *Nat. Biotechnol. 24*, 1551−1557.

(9) Henzler-Wildman, K. A., Lee, D.-K., and Ramamoorthy, A. (2003) Mechanism of lipid bilayer disruption by the human antimicrobial peptide, LL-37. *Biochemistry 42*, 6545−6558.

(10) Yandek, L. E., Pokorny, A., Florén, A., Knoelke, K., Langel, Ü., and Almeida, P. F. F. (2007) Mechanism of the Cell-Penetrating Peptide Transportan 10 Permeation of Lipid Bilayers. *Biophys. J. 92*, 2434−2444.

(11) Fry, D. W., White, J. C., and Goldman, I. D. (1978) Rapid separation of low molecular weight solutes from liposomes without dilution. *Anal. Biochem. 90*, 809−815.

(12) Mawuenyega, K. G., Forst, C. V., Dobos, K. M., Belisle, J. T., Chen, J., Bradbury, E. M., Bradbury, A. R. M., and Chen, X. (2005) *Mycobacterium tuberculosis* functional network analysis by global subcellular protein profiling. *Mol. Biol. Cell 16*, 396−404.

(13) Tsao, H. S., Spinella, S. A., Lee, A. T., and Elmore, D. E. (2009) Design of novel histone-derived antimicrobial peptides. *Peptides 30*, 2168−2173.

(14) Henzler-Wildman, K. A., Martinez, G. V., Brown, M. F., and Ramamoorthy, A. (2004) Perturbation of the Hydrophobic Core of Lipid Bilayers by the Human Antimicrobial Peptide LL-37. *Biochemistry 43*, 8459−8469.

(15) Hilpert, K., Elliott, M. R., Volkmer-Engert, R., Henklein, P., Donini, O., Zhou, Q., Winkler, D. F. H., and Hancock, R. E. W. (2006) Sequence requirements and an optimization strategy for short antimicrobial peptides. *Chem. Biol. 13*, 1101−1107.

(16) Brennan, P. J., and Nikaido, H. (1995) The envelope of mycobacteria. *Annu. Rev. Biochem. 64*, 29−63.

(17) Cheng, J. T. J., Hale, J. D., Elliott, M., Hancock, R. E. W., and Straus, S. K. (2011) The importance of bacterial membrane composition in the structure and function of aurein 2.2 and selected variants. *Biochim. Biophys. Acta 1808*, 622−633.

(18) Bryksa, B. C., MacDonald, L. D., Patrzykat, A., Douglas, S. E., and Mattatall, N. R. (2006) A C-terminal glycine suppresses production of pleurocidin as a fusion peptide in *Escherichia coli*. *Protein Expression Purif. 45*, 88−98.

(19) Oren, Z., and Shai, Y. (1998) Mode of action of linear amphipathic $\alpha$-helical antimicrobial peptides. *Biopolymers 47*, 451−463.

(20) Huang, H. W. (2000) Action of antimicrobial peptides: Two-state model. *Biochemistry 39*, 8347−8352.

(21) Huang, H. W. (2006) Molecular mechanism of antimicrobial peptides: The origin of cooperativity. *Biochim. Biophys. Acta 1758*, 1292−1302.

(22) Matsuzaki, K., Murase, O., Fujii, N., and Miyajima, K. (1996) An antimicrobial peptide, magainin 2, induced rapid flip-flop of phospholipids coupled with pore formation and peptide translocation. *Biochemistry 35*, 11361−11368.

(23) Powers, J.-P. S., and Hancock, R. E. W. (2003) The relationship between peptide structure and antibacterial activity. *Peptides 24*, 1681−1691.

(24) Wu, M., Maier, E., Benz, R., and Hancock, R. E. (1999) Mechanism of interaction of different classes of cationic antimicrobial peptides with planar bilayers and with the cytoplasmic membrane of *Escherichia coli*. *Biochemistry 38*, 7235−7242.

(25) Lehrer, R. I., Barton, A., Daher, K. A., Harwig, S. S., Ganz, T., and Selsted, M. E. (1989) Interaction of human defensins with *Escherichia coli*. Mechanism of bactericidal activity. *J. Clin. Invest. 84*, 553−561.

(26) Park, C. B., Yi, K. S., Matsuzaki, K., Kim, M. S., and Kim, S. C. (2000) Structure-activity analysis of buforin II, a histone H2A-derived antimicrobial peptide: The proline hinge is responsible for the cell-penetrating ability of buforin II. *Proc. Natl. Acad. Sci. U.S.A. 97*, 8245−8250.

(27) Subbalakshmi, C., and Sitaram, N. (1998) Mechanism of antimicrobial action of indolicidin. *FEMS Microbiol. Lett. 160*, 91−96.

(28) Ponpuak, M., Davis, A. S., Roberts, E. A., Delgado, M. A., Dinkins, C., Zhao, Z., Virgin, H. W., Kyei, G. B., Johansen, T., Vergne, I., and Deretic, V. (2010) Delivery of cytosolic components by autophagic adaptor protein p62 endows autophagosomes with unique antimicrobial properties. *Immunity 32*, 329−341.